

# Diffusion Bonding of Ti-6Al-4V Sheet with Ti-6Al-4V Foam for Biomedical Implant Applications

BRITTANY HAMILTON, SCOTT OPPENHEIMER, DAVID C. DUNAND,  
and DANIEL LEWIS

Advanced metallic bone implants are designed to have a porous surface to improve osseointegration and reduce risks of loosening. An alternative approach to existing surface treatments to create a porous surface is to bond separately produced metallic foams onto the implant. To assess the feasibility of this approach, a Ti-6Al-4V foam was diffusion bonded onto bulk Ti-6Al-4V in an argon atmosphere at temperatures between 1173 K and 1223 K (900 °C and 950 °C) for times between 45 and 75 minutes. These specimens were tested in tension to determine bond quality: failures occurred in the foam, indicating a strong diffusion-bonded interface. The quality of the bond was confirmed by metallographic studies, indicating that this approach, which can also be applied to creating of sandwich with porous cores, is successful.

DOI: 10.1007/s11663-013-9942-5

© The Minerals, Metals & Materials Society and ASM International 2013

## I. INTRODUCTION

HUNDREDS of thousands of biomedical devices are implanted into patients each year and, with an increasingly active population, patients are receiving orthopedic implants at younger ages. Implant osseointegration (the ability of the implant to form a lasting bond with the body cells and tissues) must be improved to avoid implant loosening and subsequent removal, especially for uncemented implants.<sup>[1]</sup> Currently, there are many areas of research focusing on improving osseointegration in biomedical implant devices. Common techniques include mechanical surface treatments, chemical surface treatments, physical deposition of material onto the surface, and the attachment of porous coatings by a variety of processes.<sup>[1–5]</sup>

Recently, a new technique was developed to create Ti-6Al-4V foams<sup>[6]</sup> by entrapping argon gas during the high-pressure densification of a powder preform, and subsequently expanding the gas within the solid, creeping Ti-6Al-4V in vacuum.<sup>[6–10]</sup> This method allows for tailored porosity and pore size. These titanium alloy foams can be used in the aerospace industry as lightweight structural panels consisting of a porous core with two fully

dense face sheets. Ti-6Al-4V has become the preferred metallic material for orthopedic devices due to its high strength, low density, and biocompatibility.<sup>[11,12]</sup> For biomedical applications, Ti-6Al-4V foams further provide a reduction in stiffness important to reduce stress shielding, and an open porosity allowing for osseointegration.

The aim of this study is to demonstrate that direct bonding of a Ti-6Al-4V foam (produced in a prior step in a controlled manner) onto bulk Ti-6Al-4V is an alternative to existing implant surface treatments.<sup>[13–16]</sup> A series of specimens with embedded metallic foam were fabricated by diffusion bonding in a thermo-mechanical simulator. Mechanical testing and microscopy characterization were performed to determine bond quality. The structural integrity and fracture surfaces of the metallic foam were also evaluated.

## II. EXPERIMENTAL

### A. Materials

The materials used in this diffusion bonding study were Ti-6Al-4V sheet and Ti-6Al-4V metallic foam. The fully dense Ti-6Al-4V sheet was received in the annealed condition from Timet (Dallas, Texas). The material was sectioned into dog-bone shaped tensile bars, 114 mm in length, 6.35 mm in thickness. In the as-received state (Figure 3, left), the average volume fraction of the beta phase was 15 pct, ranging between 10 pct and 30 pct within the material, and the average grain size was 10  $\mu\text{m}$ . The platelike alpha grains are on average 5 to 10  $\mu\text{m}$  wide and 65 to 100  $\mu\text{m}$  long in the foam (Figure 3, right).

The Ti-6Al-4V foam, with an open porosity of 45 pct, was produced by the argon entrapment and expansion method described above.<sup>[6]</sup> A foam specimen was machined to have the same cross-section as the tensile bars of 6.35 by 3.81 mm. The length was cut to 12.7 mm. After machining with a low speed diamond

---

BRITTANY HAMILTON, Research Assistant, and DANIEL LEWIS, Associate Professor, are with the Department of Materials Science and Engineering, Rensselaer Polytechnic Institute, Troy, NY 12180. Contact e-mail: lewisd2@rpi.edu SCOTT OPPENHEIMER, formerly Research Assistant with the Department of Materials Science and Engineering, Northwestern University, Evanston, IL, is now Materials Scientist with the General Electric Corporation, Niskayuna, NY. DAVID C. DUNAND, James N. and Margie M. Krebs Professor of Materials Science and Engineering, is with the Department of Materials Science and Engineering Northwestern University.

This paper is based on a thesis submitted by B. Hamilton to the Graduate Office of Rensselaer Polytechnic Institute in partial fulfillment of the requirements for the degree of Master of Science in Materials Science and Engineering.

Manuscript submitted August 2, 2012.

Article published online October 8, 2013.

saw, the foam was ultrasonically cleaned in ethanol followed by deionized water and dried with compressed air. In the as-received condition, the foam was characterized by pore sizes ranging between 100 and 400  $\mu\text{m}$  and a microstructure containing coarse, platelike alpha grains, and intergranular beta phase.

Average grain size measurements were recorded both prior to and subsequent to bonding of the titanium alloy bulk according to the ASTM E112-96 standard. Trends in the grain size across bonding conditions were observed using the comparison method as stated in the previously listed standard. Additionally, volume fraction measurements were performed using the ASTM E562-05 standard for determining volume fraction by systematic manual point count. A grid containing 70 intersections was overlaid on micrographs examined for each bonding condition.

### B. Diffusion Bonding

Tensile test specimens with embedded metallic foam were fabricated by diffusion bonding. Diffusion bonding was conducted using a Gleeble 1500D thermo-mechanical simulator (Dynamic Systems Inc., Poestenkill, NY). Each dense Ti-6Al-4V tensile bar was cut in half, and the two halves were held in place by Cu-Cr wedge-shaped grips and locking nuts in the jaws of the Gleeble. The foam specimen was inserted between the two dense halves and diffusion bonded as described later. To minimize surface roughness of the two bonding surfaces, the halved specimens were metallographically prepared by grinding down to 600 grit with SiC paper. The surfaces were cleaned with ethanol and all further handling was performed with the use of gloves and tweezers to prevent surface contamination.

The Gleeble chamber was evacuated and then subsequently backfilled with ultra high purity argon (dew point of  $-70\text{ }^\circ\text{C}$ ). This procedure was repeated three times. The argon was left to bleed into the chamber while the diffusion bonding run was completed.

The Gleeble heats the specimens resistively and requires the attachment of thermocouple wires prior to bonding. Calibrated Cr-Al type 'K' fine wire (0.254 mm diameter) thermocouples were used to control and measure the bonding temperature. Based on an application developed by Dynamic Systems Inc., a drilling and staking method was used for thermocouple attachment. The thermocouple wires were fitted into a drilled hole in the Ti-6Al-4V bar and the material around the hole was staked to keep the wires in place, as shown in Figure 1. The typical specimen setup in the Gleeble is shown in Figure 2.

The average heating rate for the diffusion bonding of the Ti-6Al-4V elements was 3 K/s (3.0  $^\circ\text{C/s}$ ). This heating rate was slow enough that the physical integrity of the metallic foam was not compromised. After initial heating to 1173 K, 1198 K, or 1223 K (900  $^\circ\text{C}$ , 925  $^\circ\text{C}$ , or 950  $^\circ\text{C}$ ), the Ti-6Al-4V specimens were held at temperature for a bonding time of 45, 60, or 75 minutes, under a compressive stress of 5 MPa. Samples were allowed to "furnace" cool within the Gleeble. Table I shows the testing parameters for the diffusion bonding experiments for the Ti-6Al-4V bulk and foam couples. A general reference to heat treatments in Ti alloys can be found in the literature.<sup>[17]</sup>

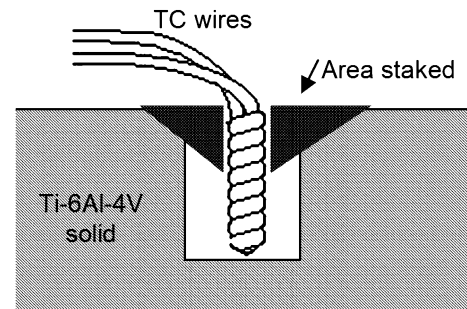


Fig. 1—Schematic of the thermocouple geometry used to attach the thermocouple wires.

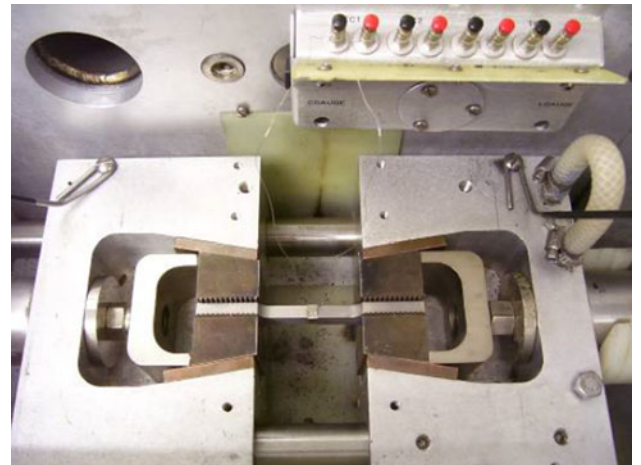


Fig. 2—The typical apparatus set-up in the Gleeble chamber for the Ti-6Al-4V bulk with the Ti-6Al-4V foam prior to bonding.

**Table I. Processing Conditions for the Diffusion Bonding of Ti-6Al-4V bulk With Ti-6Al-4V Foam**

Bonding Condition	Bonding Time (min)	Bonding Temperature [K ( $^\circ\text{C}$ )]
1	60	1173 (900)
2	75	1173 (900)
3	45	1198 (925)
4	60	1198 (925)
5	75	1198 (925)
6	45	1123 (950)
7	60	1123 (950)

Four samples were bonded at each of the bonding conditions. The stress was constant at 5 MPa. Samples were "furnace" cooled in the Gleeble.

### C. Metallurgical Preparation

Both the as-received and the diffusion bonded Ti-6Al-4V samples were prepared for metallographic examination. Samples were ground with 240, 400, and 600 grit SiC paper using standard metallographic procedures. Samples were then polished on a canvas cloth with 9  $\mu\text{m}$  diamond solution on a rotating wheel for 1 minute and on a medium nap cloth with 0.3  $\mu\text{m}$  alumina powder and a small amount of  $\text{H}_2\text{O}_2$  on a rotating wheel for

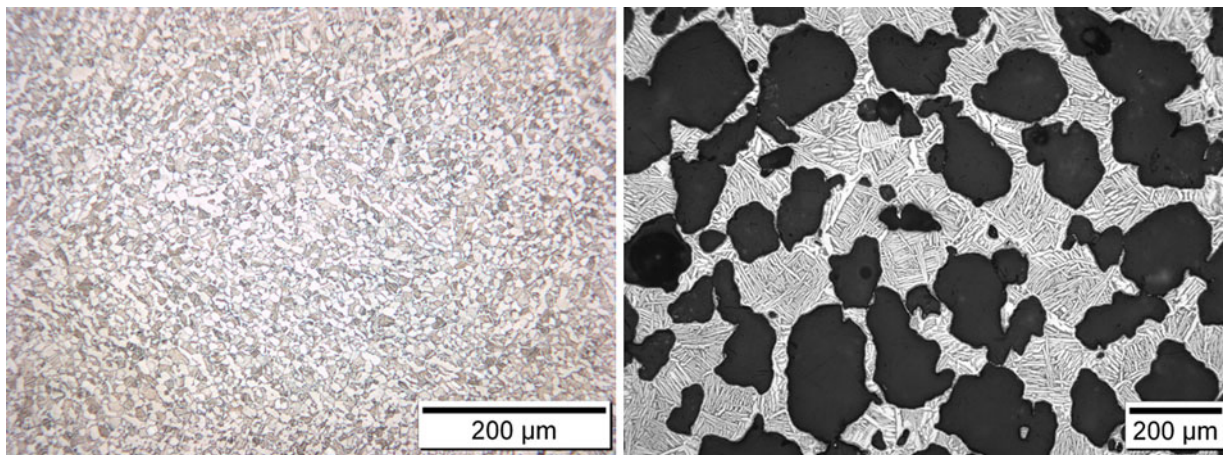


Fig. 3—Optical micrograph of Ti-6Al-4V bulk (left) and foam (right) before bonding showing pore size and connectivity within the foam.

2 minutes. All samples were etched by immersion in Kroll's etchant (100 mL H<sub>2</sub>O, 1 to 3 mL HF, and 2 to 6 mL HNO<sub>3</sub> for 10 to 15 seconds (Figure 3).

### III. RESULTS

Figure 4 is an secondary electron micrograph showing the interconnected porous network of the foam. This figure shows facets and the hexagonal structure of the foam created during the foaming process.

All of the diffusion bonded interfaces examined with microstructural analysis showed bonding between the foam and the bulk. Two parameters were used to characterize the diffusion bonded interface. An estimate of the quality of the bonded interface, formed between the Ti-6Al-4V bulk and foam, was determined using light optical microscopy (LOM) and visual examination. This bonding fraction was determined as the ratio of  $L_B$ , the length of interface that shows bonding, to  $L_T$ , the total available interface length.

Micrographs of cross-sections of the diffusion bonded interfaces for bonding conditions 2, 3, 5, and 7 are presented in Figure 5. In Figures 5(a) and 5(b), voids are observed at the interface and minimal growth of alpha grains is noted across the interface. The diffusion bonded interface for bonding condition 5, displayed in Figure 5(c) shows near-complete diffusion bonding across the interface of the foam and the bulk. The bond line is difficult to identify visually. Grain growth at the interface of both the alpha phase and the beta phase is observed.

Figure 5(d) shows the interface after diffusion bonding at bonding condition 7. The micrograph shows a nearly uniform microstructure across the interface with few interfacial voids observed. There is growth of both the alpha and beta phase across the interface. Along with the sample bonded at bonding condition 6 [at the highest temperature of 1223 K (950 °C)], the microstructure of the bulk at bonding condition 7 shows marked grain growth. The size of the beta grains was 10 μm in the as-received material, but after bonding, these beta grains grew to a size range between 80 and 1,000 μm. For the materials bonded at bonding

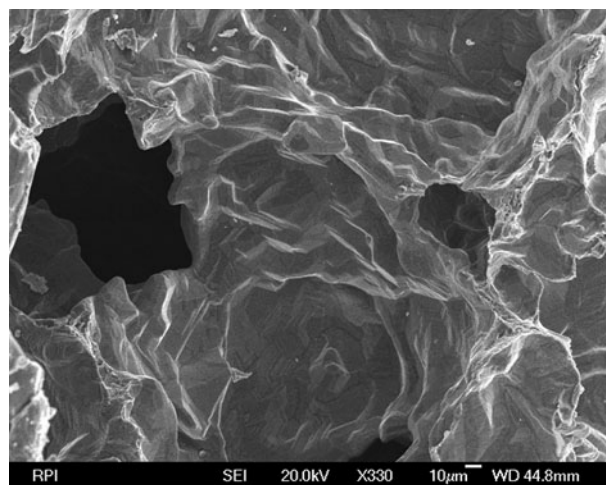


Fig. 4—Secondary electron micrograph of Ti-6Al-4V foam before bonding showing the interconnected porous network of the foam.

conditions 1 to 5, the microstructures of both the foam and the bulk are qualitatively unchanged when compared to the as-received materials.

Once the tensile test specimens were fabricated by diffusion bonding, tensile testing was performed using an Instron 8562. The mechanical properties of three samples fabricated at each of the seven bonding conditions were assessed through measurement of the tensile strength. A strain rate of 0.5 mm/min was used. The average tensile strength of the samples across all seven bonding conditions was  $105 \pm 15$  MPa. As expected for metallic foams in tension, very little tension ductility was observed. Results from microstructural analysis and mechanical testing for all seven bonding conditions are presented in Table II.

Figure 6 shows the fracture surface of a diffusion bonded Ti-6Al-4V sample, at bonding condition 4, from two perspectives. In all samples, the tensile failures occurred in the foam, as shown in Figure 6(a), not at the diffusion bonded bulk/foam interface. Additionally, for many of the foam fracture surfaces, an oxide casing was observed on the outer perimeter of the foam. The

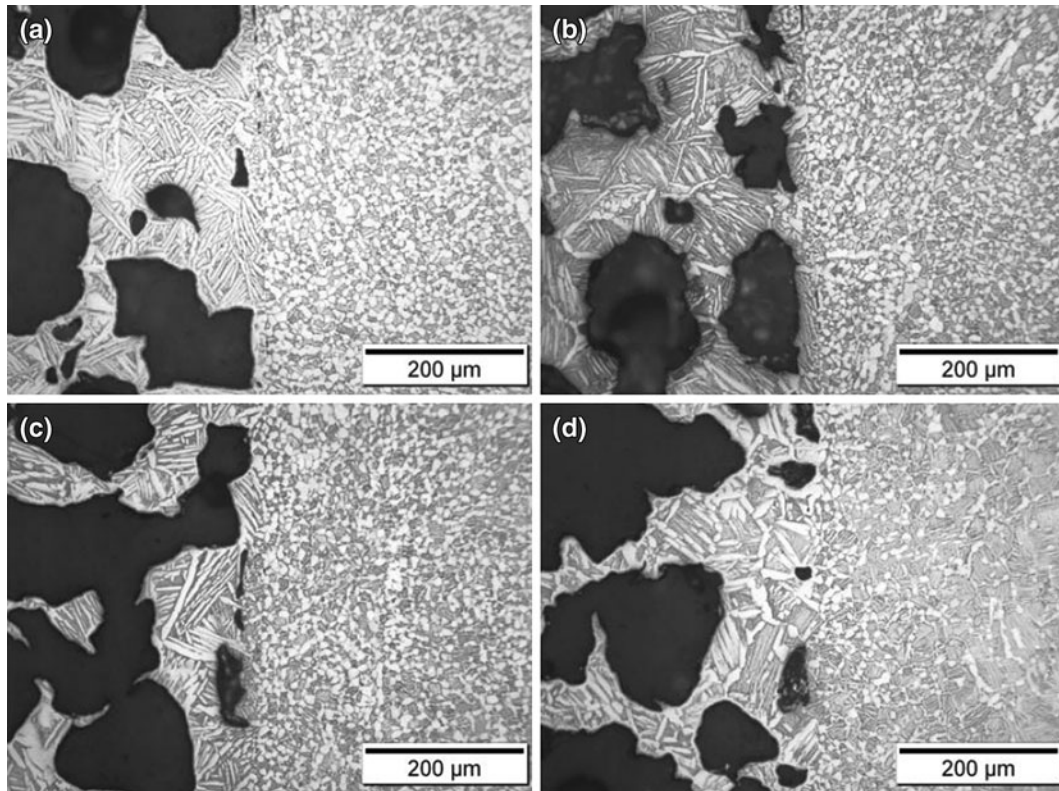


Fig. 5—Optical micrographs of the diffusion-bonded interfaces between the Ti-6Al-4V bulk and foam at bonding conditions (a) 2, (b) 3, (c) 5, and (d) 7.

**Table II. Results from Bonding Characterization and Mechanical Testing from all Seven Bonding Conditions**

Bonding Condition	Bonding Fraction (Pct)	Tensile Strength (MPa)
1	87	116
2	84	80
3	90	107
4	91	95
5	94	105
6	97	110
7	93	116

One sample for each bonding condition was prepared for microstructural analysis and three samples for each bonding condition were prepared for mechanical testing. Listed above are the average bond line percentages and tensile strengths for specimens at each bonding condition.

thickness of the oxide casing, shown in Figure 6(c) ranged between 500 and 1,800  $\mu\text{m}$ .

Examination of the Ti-6Al-4V foam fracture surfaces showed features characteristic of both brittle and ductile failure modes. Two scanning electron microscopy (SEM) secondary electron images of the foam fracture surface are presented in Figure 7. Figure 7(a) shows regions of microvoids and tear ridges, characteristics of ductile failure, as well as cleavage facets, characteristics of brittle failure. The micrograph in Figure 7(b) clearly presents regions of fracture ridges, dimples, and microvoids alternating with regions of cleavage facets and transgranular cracks.

#### IV. DISCUSSION

All Ti-6Al-4V samples showed mechanical and metallurgical bonding upon removal from the Gleeble chamber. It is apparent that all of the samples exhibit comparable tensile strengths, with an average of 105 MPa across all seven conditions. This strength exceeds the minimum tensile strength of 20 MPa recommended by the US Food and Drug Administration (USFDA) in an Implant Guidance Document for metallic coatings on orthopedic implant devices.<sup>[18]</sup> For each bonding condition, the strength of the interface was greater than that of the foam itself, as all of the failures occurred in the foam.

An estimate of the quality of the bonded interface formed between the titanium alloy bulk and foam was determined based on microscopic examination. The length of interface showing no unbonded interfacial region was divided by the total measured interface length in order to develop a parameter for estimating bond quality. This parameter is reported as a percent of the available interface distance. The bonding fraction measurements show that in all cases, more than 80 pct of the total available interface distance exhibited visible bonding.

Both bonding conditions 6 and 7 resulted in diffusion bonded interfaces with the highest bonding fraction; however, the observed microstructural changes in the bulk are undesirable. The bulk microstructure contains beta grains scaled between 150 and 1,000  $\mu\text{m}$ , a 10 to 100-fold increase from the

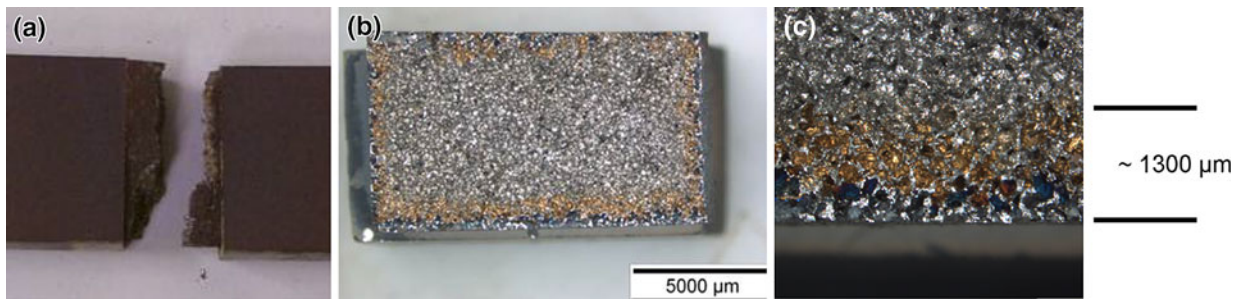


Fig. 6—Fracture surfaces of a diffusion bonded Ti-6Al-4V specimen, at bonding condition 4, from two perspectives: (a) side view, (b) top view, and (c) a higher magnification top view, illustrating the oxide growth.

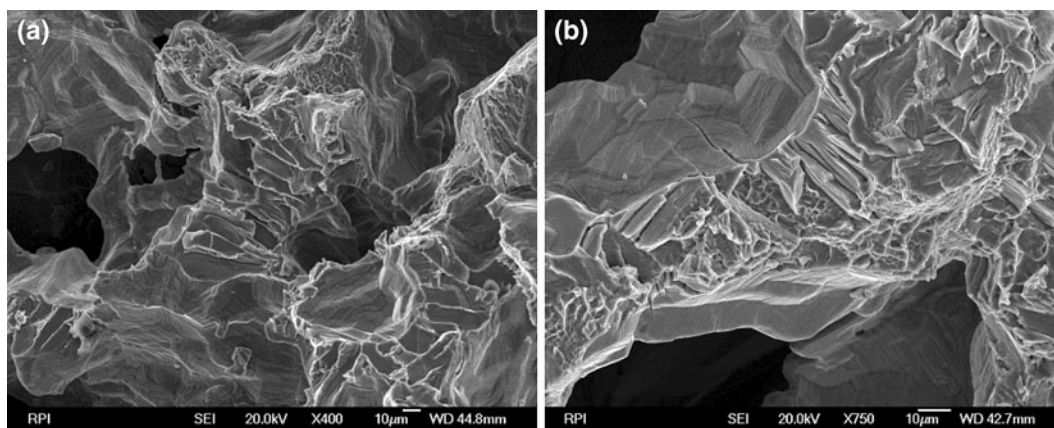


Fig. 7—Secondary electron micrographs of the Ti-6Al-4V fracture surfaces at (a) bonding condition 5 and (b) bonding condition 7. Both micrographs show features characteristic of brittle and ductile failure.

as-received grain size of  $10\ \mu\text{m}$ . This nonuniform microstructure will result in decreased strength, fatigue, and hardness properties compared to the as-received material. The microstructural change was likely caused by uneven heating of the sample or difficulties resulting from the attachment of the thermocouple wires. A complete microstructural transformation was not observed and the bonding temperature for these two bonding conditions was  $1223\ \text{K}$  ( $950\ ^\circ\text{C}$ ) below the  $1263\ \text{K}$  ( $990\ ^\circ\text{C}$ ) beta transus of the alloy. Microstructural uncertainty, as seen in bonding conditions 6 and 7, can be problematic for materials in biomedical applications.

Based on the results from mechanical testing and microstructural observations, bonding performed at  $1198\ \text{K}$  ( $925\ ^\circ\text{C}$ ) for 75 minutes (bonding condition 5) presents an optimal diffusion bonded interface. As stated previously, the tensile strength of both the Ti-6Al-4V foam and the Ti-6Al-4V bulk are well above the recommended value of  $20\ \text{MPa}$ .<sup>[20]</sup> Additionally, the microstructural observations show a bonding fraction of 95 pct across the interface. The microstructure presented in Figure 5(c) shows the uniform microstructure of a continuously bonded interface. Image analysis conducted over eight fields shows that the volume fraction of the beta phase increased from 15 pct in the as-received condition to 19 pct in the bonding condition 5. The observed volume fraction after bonding is still

within the range of volume fractions reported earlier for the as-received material.

Furthermore, for the temperature and times used here, the relatively low stress of  $5\ \text{MPa}$  did not lead to appreciable plastic deformation of the Ti-6Al-4V foam. The pore size and microstructure of the foam after bonding are qualitatively unchanged when compared to the as-received foam. The pore size continues to range between  $100$  and  $400\ \mu\text{m}$ . Many studies have concluded that pore sizes between  $50\ \mu\text{m}$  and  $400\ \mu\text{m}$  are preferred for biomedical applications.<sup>[19–22]</sup> Additionally, one study suggested that a pore size greater than  $150\ \mu\text{m}$  was required for osseointegration.<sup>[23]</sup> The Ti-6Al-4V metallic foam used for this research falls within these recommended parameters.

The fracture surfaces presented in the SEM micrographs above contain features characteristic of both ductile and brittle fracture modes. Bulk Ti-6Al-4V does not have a characteristic ductile to brittle transition temperature and tensile fracture surfaces typically show dimpling, a characteristic of ductile failure. Alternatively, due to the porous structure of metallic foams, foam tensile fracture surfaces are typically characterized as brittle. The pores in the foam act as notches and stress concentrators upon tensile loading, and the resulting triaxial stresses induce brittle failure. Upon further examination of the fracture surfaces and comparison with the microstructure of the foam, the geometry and scale of the cleavage facets

in the fracture surface correspond to the same geometry and scale of the alpha phase in the microstructure. This suggests that the alpha phase fails by brittle fracture. The fractograph in Figure 7(a) clearly presents these cleavage facets. The regions between the facets appear to show ductile behavior and, upon comparison with the microstructure of the foam, this suggests that the beta phase fails by ductile fracture.

Additionally, there is no metallurgical evidence that the native TiO<sub>2</sub> layer on the surface of the Ti-6Al-4V materials inhibited the diffusion bonding.<sup>[24]</sup> An increase in the surface oxide thickness was observed on the samples after bonding; however, there was no evidence of an oxygen-rich alpha casing in the microstructure of either the bulk or the foam during analysis. The oxidation did not inhibit diffusion bonding across the interface; however, an alternative inert atmosphere with additional backfilling steps may help to decrease the oxidation on the surfaces of both the bulk and the foam.

## V. CONCLUSIONS

A series of diffusion bonding experiments between bulk Ti-6Al-4V and a Ti-6Al-4V foam were performed at 1173 K to 1223 K (900 °C to 950 °C) for 45 to 75 minutes in an argon atmosphere. The stress of 5 MPa was too low to cause plastic deformation of the foam but sufficiently high to produce a diffusion bonded interface with up to 95 pct bonding fraction. The foam had an average tensile strength of 105 MPa, well beyond the 20 MPa minimum tensile strength requirement for orthopedic implants<sup>[18]</sup> and in excess of the bulk/foam interface fracture stress. For the lower bonding temperature range, the microstructures of both the bulk and foam materials are qualitatively unchanged after the bonding procedure.

The as-received foam displayed a pore size between 100 μm and 400 μm and a microstructure containing coarse, platelike alpha grains and intergranular beta phase. Upon tensile loading, the Ti-6Al-4V foam displayed features attributed to both ductile and brittle failure.

## REFERENCES

1. Y. Yang, N. Oh, Y. Liu, W. Chen, S. Oh, M. Appleford, S. Kim, K. Kim, S. Park, J. Bumgardner, W. Haggard, and J. Ong: *JOM*, 2006, vol. 58, pp. 71–76.
2. J.R. Davis, ed.: *Handbook of Materials for Medical Devices*, ASM International, Materials Park, OH, 2003, pp. 179–94.
3. Y.Z. Yang, J.M. Tian, Z.Q. Chen, X.J. Deng, and D.H. Zhang: *J. Biomed. Mater. Res.*, 2000, vol. 52, pp. 333–37.
4. H.B. Wen, J.R. de Wijn, F.Z. Cui, and K. de Groot: *Biomaterials*, 1998, vol. 19, pp. 215–21.
5. J. Lincks, B.D. Boyan, C.R. Blanchard, C.H. Lohmann, Y. Liu, D.L. Cochran, D.D. Dean, and Z. Schwartz: *Biomaterials*, 1998, vol. 19, pp. 2219–32.
6. M.W. Kearns, P.A. Blenkinsop, A.C. Barber, and T.W. Farthing: *Int. J. Powder Metall.*, 1988, vol. 24, pp. 59–64.
7. D.C. Dunand: *Adv. Eng. Mater.*, 2004, vol. 6, pp. 369–76.
8. J. Banhart: *Prog. Mater. Sci.*, 2001, vol. 46, pp. 559–632.
9. D.T. Queheillalt, B.W. Choi, D.S. Schwartz, and H.N.G. Wadley: *Metall. Mater. Trans. A*, 2000, vol. 31A, pp. 261–73.
10. N.G.D. Murray and D.C. Dunand: *Compos. Sci. Technol.*, 2003, vol. 63, pp. 2311–16.
11. M. Long and H.J. Rack: *Biomaterials*, 1998, vol. 19, pp. 1621–39.
12. W.C. Head, D.J. Bauk, and R.H. Emerson: *Clin. Orthop. Relat. Res.*, 1995, vol. 311, pp. 85–90.
13. M. W. Mahoney and C. C. Bampton: *Welding, Brazing and Soldering, ASM Handbook*, vol. 6, ASM International, Materials Park, OH, 1995, pp. 156–59.
14. D.G. Sanders and M. Ramulu: *J. Mater. Eng. Perform.*, 2004, vol. 13, pp. 744–52.
15. H.S. Lee, J.H. Yoon, and Y.M. Yi: *Thermochim. Acta*, 2007, vol. 455, pp. 105–08.
16. S.J. Tuppen, M.R. Bache, and W.E. Voice: *Mater. Sci. Technol.*, 2006, vol. 22, pp. 1423–30.
17. G. Lutjering and J.C. Williams: *Titanium*, 2nd ed., Springer, New York, 2007.
18. US Food and Drug Administration: *Guidance Document for Testing Orthopedic Implants with Modified Metallic Surfaces Apposing Bone or Bone Cement*, Office of Device Evaluation, Center for Devices and Radiological Health, April 28, 1994.
19. S.F. Hulbert, S.J. Morrison, and J.J. Klawitter: *J. Biomed. Mater. Res.*, 1972, vol. 6, pp. 347–74.
20. H. Li, S.M. Oppenheimer, S.I. Stupp, D.C. Dunand, and L.C. Brinson: *Mater. Trans., JIM*, 2004, vol. 45, pp. 1124–31.
21. E.D. Spoerke, N.G. Murray, H. Li, L.C. Brinson, D.C. Dunand, and S.I. Stupp: *Acta Biomater.*, 2005, vol. 1, pp. 523–33.
22. A. Schuh, J. Luyten, R. Vidael, W. Honle, and T. Schmickal: *Materialwiss. Werkstofftech.*, 2007, vol. 38, pp. 1015–18.
23. J.D. Bobyn, R.M. Pilliar, H.U. Cameron, and G.C. Weatherly: *Clin. Orthop. Relat. Res.*, 1980, vol. 150, pp. 263–70.
24. Y. Mizuno, F.K. King, Y. Yamauchi, T. Homma, A. Tanaka, Y. Takakuwa, and T. Momose: *J. Vac. Sci. Technol. A*, 2002, vol. 20 (5), pp. 1716–21.